HYPR-Constrained Compressed Sensing Reconstruction for Accelerated Time Resolved Imaging

H. Wu[1], W. F. Block[1,2], and A. A. Samsonov[1]

[1]Medical Physics, University of Wisconsin-Madison, Madison, Wisconsin, United States, [2]Biomedical Engineering, University of Wisconsin-Madison, Madison, Wisconsin, United States

Introduction: The sparse nature of CE-MRA data has been a basis for accelerating time resolved imaging with non-Cartesian trajectories through undersampling. The mild appearance of undersampling artifacts with 2D and 3D radial trajectories has allowed acceleration factors up to 6 and 20, respectively. It has been recently demonstrated that the sparsity of such data may provide a basis for much larger acceleration factors, if special reconstruction techniques are applied. One such technique, HighlY constrained Projection (HYPR), has demonstrated acceleration factors on the order of 100 [1]. Artifacts of HYPR reconstruction have been reduced in HYPR Local Reconstruction (HYPR LR) and its iterative extensions [2-4]. HYPR and HYPR LR, which rely on *a priori* information from a composite image to reconstruct individual time frames, provide a reasonable tradeoff between reconstruction speed and accuracy. The drawbacks of these approximate methods are that they are not readily extendable to accommodate traditional acceleration mechanisms such as parallel imaging and temporal filtering. We now extend HYPR Reconstruction by Iterative Estimation (HYPRIT) [6-7], an iterative HYPR method that utilizes compressed sensing [5], to incorporate parallel imaging and speeds convergence by using an improved constraining estimate. We also demonstrate the reduced reconstruction errors in HYPRIT in applications in time-resolved CE-MRA relative to a non-iterative reconstruction.

Theory and Methods: In HYPRIT, the image **f** is sought to minimize $\|\mathbf{Ef}-\mathbf{s}\|_2 + \lambda\|\mathbf{f}-\mathbf{f}_S\|_1$, where **E** is the encoding matrix, **s** is the data vector, and $\mathbf{f}_S$ is the constraining or *sparsifying* image in context of compressed sensing formalism. To promote sparsity in the iterative solution, $\mathbf{f}_S$ should be chosen to be a good approximation of the underlying time frame. The procedure may be split into two stages: obtaining the constraining image and then utilizing it in the iterative reconstruction. Here, we consider two options for the constraining image: an image from a sliding window reconstruction (termed the sliding window composite in the HYPR and HYPR LR) and the HYPR LR image. The minimization is accomplished using the method of iterative reweighting [8] and partially presented in [7].

We first built a digital phantom with the cross-section of 16 circles simulating blood vessels. 20 time frames were generated and each vessel had unique temporal waveform. A simulated acquisition consisted of 20 projections per time frame, each with a resolution of 256 points. Intensity time curves from HYPR LR images and HYPRIT images were calculated and compared. Next, a series of 50 time frames from a time resolved FGRE acquisition of a contrast injection into a carotid phantom were regarded as artifact-free images. A time-resolved radial acquisition was simulated, again with 20 projections per time frame and 256 resolution. This data was generated for a single coil and a simulated eight channel system to validate parallel imaging in HYPRIT. Lastly, HYPRIT processing was performed on a CE-MRA thigh exam of a volunteer using a 512 resolution stack of stars radial sequence with 26 slices. Here 16 time-frames were collected, each containing 16 interleaved projections at all slice encodings. The HYPRIT processing used 6 conjugate gradient (CG) iterations, 2 reweighing iterations, and was solved using CG with the gridding approximation of the DFT transform [9].

Results: Fig. 1 shows the time curve of two vessels in the first simulation that were reconstructed by HYPRIT and HYPR LR. The HYPRIT-generated curves correlate well with the true curves. HYPR LR accurately reconstructed vessel B, but altered the waveform of vessel A due to cross talk between vessels with different temporal dynamics. In the study using the carotid phantom shown in Fig. 2, HYPR LR shows some errors in early time frames characterized by rapid contrast arrival (Fig. 2c). HYPRIT, using the sliding window composite as the sparsifying image, gives errors in the early time frames due to the same reason. The errors are minimized when HYPRIT uses the HYPR LR image as a sparsifying image (Fig. 2e). Incorporating parallel imaging acceleration into HYPRIT shows the least error among all cases (Fig. 2f). Comparing the time curves, HYPR LR dampens initial enhancement slightly and depicts washout out slightly early while HYPRIT preserves the temporal information. Finally, the progression of contrast through the thigh station is shown in Fig. 3 using HYPRIT.

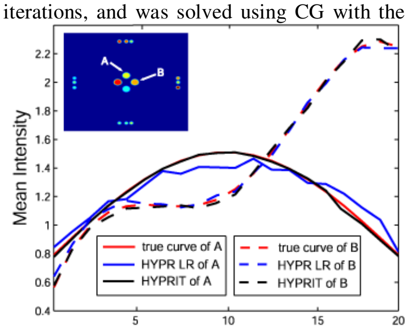

Figure 1. Time curves of vessel A and B (pointed by arrows in phantom in the upper left) demonstrates good accuracy for both methods, accuracy, but HYPRIT performs better when vessels are in close proximity.

Discussion and Conclusion: Our results show that HYPRIT may be a promising tool for accelerating CE-MRA exams. It has provided excellent preservation of temporal dynamics in simulated studies and promising results in actual studies. We have demonstrated that very high acceleration factors within good accuracy could be attained within the linear reconstruction framework. The flexibility of the framework to include additional acceleration mechanisms such as parallel imaging was shown with HYPRIT. Including such acceleration options as kt BLAST/kt SENSE [10] may be important to close to acceleration factors needed for such demanding applications as AVM imaging.

HYPR LR performed well in most situations. As HYPR LR images are usually closer to the true time frames than sliding window composite images, it could be a good strategy to use HYPR LR for a quick estimation of the sparsifying images for subsequent HYPRIT reconstructions. HYPRIT could greatly improve reconstruction accuracy in situations where HYPR LR is challenged. Thus, HYPRIT could obtain more accurate temporal information with higher SNR at an increased cost in reconstruction time. In this sense, both methods may be considered as complimentary.

Acknowledgments: This research is supported NIH NCI 1R01CA116380-01A1 and GE Healthcare.

References: [1] Mistretta et al. MRM, 55:30-40 (2006). [2] Johnson et al. MRM in press**.** [3] O' Halloran *et al.* MRM in press. [4] Griswold *et al.* MRA Workshop 2006. [5] Lustig. *et al.* MRM in press. [6] Samsonov *et al.* submitted to ISMRM 2008. [7] Samsonov *et al.* ISMRM Workshop on Non-Cart. MRI, 2007. [8] Gorodnitsky. IEEE-TSP, 45(3): 600-616 (1997). [9] Pruessmann *et al.* MRM, 46:638-651 (2001). [10] Pruessmann *et al.* MRM, (2003).

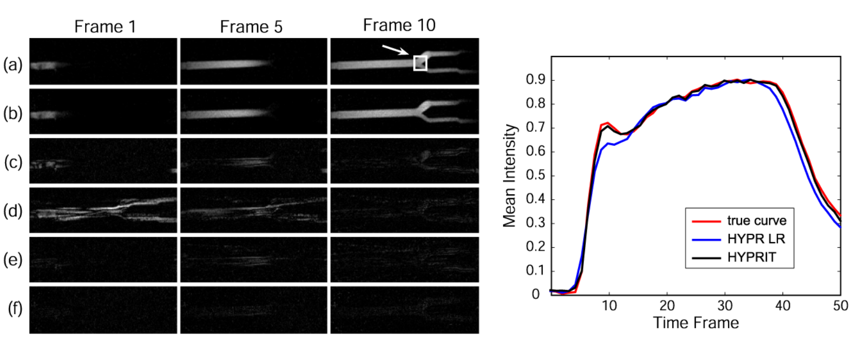

Figure 2. Carotid phantom study for select time frames. **Left: a**: true time frames. **b:** time frames of multichannel HYPRIT. **c,d,e,f:** error images (x 2.5) by HYPR-LR, HYPRIT with sliding window sparsifying image, HYPRIT and multichannel HYPRIT with HYPR LR sparsifying images, respectively. **Right:** Time curves from the ROI(arrow) by HYPR LR and HYPRIT

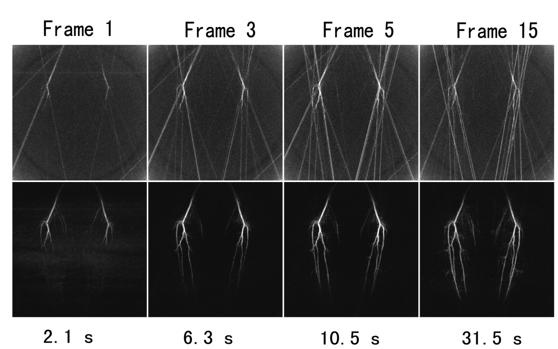

Figure 3. Time-resolved CE-MRA thigh study. **Top:** MIPs of subsampled data. **Bottom:** Corresponding MIPs of HYPRIT images demonstrates high speed femoral enhancement w/ high SNR and substantially lower artifacts.